/EtOAc) (lit. mp 113 °C);[21] ^{1}H NMR δ 9.04 (d, 1 H, J = 2.4 Hz), 8.36 (dd, 1 H, J = 2.4, 8.7 Hz), 7.57 (d, 1 H, J = 8.7 Hz), 3.08 (q, 2 H, J = 7.3 Hz), 1.46 (t, 3 H, J = 7.3 Hz); ^{13}C NMR δ 147.29, 144.59, 143.60, 126.98, 126.75, 121.65, 26.71, 12.44; IR (film) 3098, 2986, 1589, 1516, 1451, 1344, 1308, 1246, 154, 1098, 1053, 921, 832, 734 cm^{-1}; GC-MS m/e (%) 228 (M^+, 59), 200 (16), 184 (30), 183 (100), 137 (16), 106 (20), 95 (28), 91 (17), 79 (28), 77 (16), 69 (38), 63 (52), 62 (16).

Acknowledgment. We thank Shu Hai Zhao and Mohan Thiruvazhi for experimental assistance and gratefully acknowledge support from the donors of the Petroleum Research Fund, administered by the American Chemical Society, the Herman Frasch Foundation, the National Science Foundation, and Société Nationale Elf Aquitaine.

Registry No. 1a, 81788-92-3; **1b**, 139631-56-4; **1c**, 139631-57-5; **1d**, 139631-59-7; **2a**, 64251-85-0; **2b**, 33945-99-2; **2c**, 139631-58-6; **2d**, 76832-59-2; **3**, 139631-66-6; **3a**, 139631-71-3; **3b**, 139631-72-4; **4**, 6863-32-7; **5**, 139631-60-0; **6**, 68846-57-1; **7**, 139631-61-1; **8**, 139631-62-2; **9**, 139631-63-3; **10**, 74379-74-1; **11**, 139631-65-5; **12**, 139631-68-8; **13**, 139631-69-9; **14**, 139631-70-2; **15**, 7343-55-7; **18**, 139631-64-4; **19**, 139631-67-7; sulfene, 917-73-7; bromocyclopropane, 4333-56-6.

^{13}C-^{13}C Spin Coupling Constants in Aldoses Enriched with ^{13}C at the Terminal Hydroxymethyl Carbon: Effect of Coupling Pathway Structure on J_{CC} in Carbohydrates

Jian Wu,[†] Paul B. Bondo,[‡] Tapani Vuorinen,[§] and Anthony S. Serianni*,[†]

Contribution from the Department of Chemistry and Biochemistry, University of Notre Dame, Notre Dame, Indiana 46556, Omicron Biochemicals, Inc., 19882 Alou Lane, South Bend, Indiana 46637, and Laboratory of Wood Chemistry, Helsinki University of Technology, SF-02150 Espoo, Finland. *Received July 31, 1991*

Abstract: Eight aldohexoses (allo, altro, galacto, gluco, gulo, ido, manno, talo), four aldopentoses (arabino, lyxo, ribo, xylo), and two aldotetroses (erythro, threo) have been prepared with ^{13}C-enrichment (99 atom-% ^{13}C) at the terminal hydroxymethyl (CH_2OH) carbon. High-resolution ^{1}H-decoupled ^{13}C NMR spectra were obtained at 75 and 125 MHz in order to obtain one-bond ($^1J_{CC}$) and longer range ($^2J_{CC}$, $^3J_{CC}$) ^{13}C-^{13}C spin coupling constants involving the terminal carbons of the more abundant furanose and pyranose forms of these monosaccharides in ^2H_2O. In some cases spectral interpretation was assisted by the use of one-dimensional INADEQUATE ^{13}C spectra. The effect of aldopyranose and aldofuranose ring structure and conformation on the magnitudes of these couplings, especially $^2J_{CCC}$ and $^3J_{CCCC}$, was probed. Results show that $^2J_{CCC}$ is highly affected by the orientation of terminal hydroxyl substituents along the C-C-C coupling pathway and that $^3J_{CCCC}$ is not only affected by molecular dihedral angle (i.e., Karplus relationships) but also by substituent geometry along the C-C-C-C coupling pathway.

Introduction

In recent years, nuclear magnetic resonance (NMR) spectroscopy has emerged as a powerful tool to investigate the structures and conformational features of biologically-important molecules in solution. The development of multidimensional modes of data collection[1,2] has played a dominant role in this regard, especially in studies of macromolecules such as proteins and nucleic acids. Implicit in these new methods is the fundamental assumption that an intelligent integration of different NMR parameters can lead to more reliable models of solution behavior. For example, the combined use of ^{1}H-^{1}H spin couplings (J_{HH}) and nOes, measured from COSY and NOESY spectra, respectively, has been important in computer-aided three-dimensional structure determinations of proteins.[3,4] Thus, studies aimed at an improved understanding of how specific NMR parameters are affected by molecular structure and dynamics are critical to the development of NMR-based strategies to probe the solution properties of molecules.

While numerous NMR studies of carbohydrates have used ^{1}H-^{1}H spin couplings to assess molecular structure and conformation,[5] interest in ^{13}C-^{1}H (J_{CH}) and ^{13}C-^{13}C (J_{CC}) spin couplings is increasing, partly because modern NMR methods are available that permit their measurement without the need for ^{13}C-enrichment.[6,7] Thus, while the problem of measurement has been reduced, a real need exists for systematic investigations of the dependencies of these couplings on carbohydrate structure. This need is particularly acute for J_{CC}, since it is well recognized that relatively subtle changes in structure along the coupling pathway may dramatically affect their magnitudes.[8] Seminal studies in non-carbohydrate systems conducted by Barfield and co-workers[9-11] have clearly shown that J_{CC} depends highly on pathway

[†] University of Notre Dame.
[‡] Omicron Biochemicals, Inc.
[§] Helsinki University of Technology.

(1) (a) Ernst, R. R.; Bodenhausen, G.; Wokaun, A. *Principles of Nuclear Magnetic Resonance in One and Two Dimensions*; Oxford University Press: New York, 1987. (b) *Pulse Methods in 1D and 2D Liquid-Phase NMR*; Brey, W. S., Ed.; Academic Press: New York, 1988.
(2) (a) Vuister, G. W.; de Waard, P.; Boelens, R.; Vliegenthart, J. F. G.; Kaptein, R. *J. Am. Chem. Soc.* **1989**, *111*, 772. (b) Fesik, S. W.; Gampe, R. T., Jr.; Zuiderweg, E. R. P. *J. Am. Chem. Soc.* **1989**, *111*, 770. (c) Kay, L. E.; Clore, G. M.; Bax, A.; Gronenborn, A. M. *Science* **1990**, *249*, 411.
(3) Wüthrich, K. *NMR of Proteins and Nucleic Acids*; John Wiley and Sons: New York, 1986.
(4) (a) Bax, A. *Ann. Rev. Biochem.* **1989**, *58*, 223. (b) Clore, G. M.; Gronenborn, A. M. *Crit. Rev. Biochem. Mol. Biol.* **1989**, *24*, 479.
(5) (a) For a general discussion of the use of J_{HH} in the conformational analysis of cyclic compounds, see: Booth, H. *Prog. NMR Spectrosc.* **1969**, *5*, 149. (b) Bentley, R. *Ann. Rev. Biochem.* **1972**, *41*, 953.
(6) (a) Bax, A.; Freeman, R. *J. Am. Chem. Soc.* **1982**, *104*, 1099. (b) Morat, C.; Taravel, F. R.; Vignon, M. R. *Magn. Reson. Chem.* **1988**, *26*, 264.
(7) (a) Bax, A.; Freeman, R.; Kempsell, S. P. *J. Am. Chem. Soc.* **1980**, *102*, 4849. (b) Bax, A.; Freeman, R.; Frenkiel, T. A.; Levitt, M. H. *J. Magn. Reson.* **1980**, *43*, 478.
(8) Marshall, J. L. *Carbon-Carbon and Carbon-Proton NMR Couplings: Applications to Organic Stereochemistry and Conformational Analysis*; Verlag Chemie: Weinheim/Bergstrasse, Germany, 1983.
(9) (a) Barfield, M.; Burfitt, I.; Doddrell, D. *J. Am. Chem. Soc.* **1975**, *97*, 2631. (b) Barfield, M.; Conn, S. A.; Marshall, J. L.; Miiller, D. E. *J. Am. Chem. Soc.* **1976**, *98*, 6253.
(10) Marshall, J. L.; Conn, S. A.; Barfield, M. *Org. Magn. Reson.* **1977**, *9*, 404.

0002-7863/92/1514-3499$03.00/0

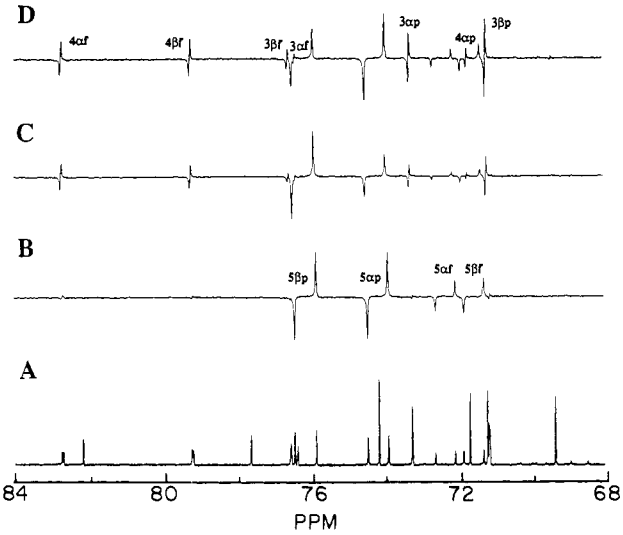

Figure 1. (A) The partial ^{1}H-decoupled ^{13}C NMR spectrum (75 MHz) of L-[6-^{13}C]idose. (B–D) INADEQUATE ^{13}C NMR spectra of L-[6-^{13}C]-idose obtained with a 6 (B), 50 (C), and 100 ms (D) mixing time. Shorter mixing times enhance the detection of carbons directly bonded to the enriched site, while longer mixing times suppress the one-bond correlations and enhance the detection of coupled carbons further removed from the enriched site. Close inspection of data in (D) reveals small couplings to C3 of the α-furanose (~76.4 ppm) and to C4 of the α-pyranose (~71.7 ppm) that were not detected in the conventional 1D spectrum in (A).

structure and that faulty interpretations can occur when these couplings are applied without a detailed knowledge of this dependency.

In a previous study,[12] we examined J_{CC} in the aldoses involving the C1 (anomeric) carbon. Results showed that the relative orientation of the hydroxyl substituents on the coupled carbons, and on carbons along the coupling pathway, significantly affects the coupling magnitude. For example, $^2J_{C1,C3}$ in aldohexopyranoses was found to be large (~4.3 Hz) in structures having O1, C1, C2, C3, and O3 coplanar, and displacing either O1 or O3 out of this plane reduced this coupling to a small or zero value. $^3J_{C1,C6}$ was found to depend on the orientation of O1 with respect to the coupling pathway, with larger couplings observed when O1, C1, O5, and C5 are coplanar.[12] While the orientation of O6 with respect to this coupling pathway is also likely to affect $^3J_{C1,C6}$ in aldohexopyranoses, this effect could not be assessed due to the inherent rotational mobility of the exocyclic C5–C6 bond.

The present investigation aims to extend this earlier work to J_{CC} involving the terminal hydroxymethyl carbons of the simple aldoses. (4-^{13}C)Aldotetroses, (5-^{13}C)aldopentoses, and (6-^{13}C)-aldohexoses have been prepared, high-resolution ^{13}C NMR spectra at 125 MHz have been obtained and analyzed, and the ^{13}C–^{13}C couplings between the terminal carbon and the remaining pyranosyl and furanosyl ring carbons have been interpreted in terms of ring structure, configuration, and conformation.

Experimental Section

Materials. Potassium (^{13}C)cyanide (K^{13}CN, 99 atom-% ^{13}C) and deuterium oxide (^2H_2O, 99 atom-% ^{2}H) were purchased from Cambridge Isotope Laboratories.

Instrumentation. Broadband ^{1}H-decoupled ^{13}C NMR spectra of (^{13}C)-enriched aldoses (~0.6 M in ^2H_2O) were obtained at 125 MHz and 21° on a Varian VXR-500 (UNITY) 500 MHz FT-NMR spectrometer located in the Lizzadro Magnetic Resonance Research Center at the University of Notre Dame. Quadrature-phase spectra were obtained with a sweep width of 7000 Hz and 54 016 real points and were zero-filled to give a final digital resolution of 0.065 Hz/pt. Observation pulses of 6 μs (~25°) were employed with a relaxation delay (RD) of 5 s to give a total interpulse time interval (acquisition time + RD) of 8.5 s, and free induction decays were processed with resolution-enhancement functions (typically sine-bell or gaussian) to improve the detection of small couplings. Spectra were referenced externally to the C1 chemical shift of β-D-(1-^{13}C)glucopyranose (97.4 ppm), and reported chemical shifts and ^{13}C–^{13}C spin couplings are accurate to ±0.1 ppm and ±0.1 Hz, respectively. High-resolution ^{1}H NMR spectra (500 MHz) were collected on the same spectrometer at 21° with sweep widths of 3400 Hz and 56K data points, giving a digital resolution of 0.061 Hz/pt. ^{1}H–^{1}H spin-coupling constants are accurate to ±0.1 Hz.

One-dimensional INADEQUATE ^{13}C NMR spectra[7a,12] at 21° in ^2H_2O were obtained on a General Electric GN-300 FT-NMR spectrometer operating in the quadrature-phase mode. FIDs were processed with exponential multiplication (EM) to yield spectra with a digital resolution of 0.075 Hz/pt.

Synthesis of (^{13}C)-Labeled Aldoses. Detailed procedures for the synthesis of the ^{13}C-labeled aldoses used in this study have been published elsewhere,[13,14] and only a brief account of the methods is given here.

D-(6-^{13}C)Glucose was prepared from 1,2-*O*-isopropylidene-α-D-*xylo*-pentodialdo-1,4-furanose and K^{13}CN as described by King-Morris et al.[15] D-(6-^{13}C)Mannose was obtained from D-(6-^{13}C)glucose by molybdate-catalyzed C2-epimerization.[16]

D-(5-^{13}C)Ribose and D-(5-^{13}C)arabinose were prepared by treatment of D-(6-^{13}C)glucose with $Pb(OAc)_4$[17] to give D-(4-^{13}C)erythrose, which was chain-extended by cyanohydrin reduction[13,14,18] to give the target labeled pentoses. D-(4-^{13}C)Erythrose was epimerized with sodium molybdate[16] to yield, after chromatography, D-(4-^{13}C)threose. D-(4-^{13}C)Threose was chain-extended by cyanohydrin reduction[13,14,18] to give, after chromatography, D-(5-^{13}C)xylose and D-(5-^{13}C)lyxose.

L-(6-^{13}C)Idose was prepared from 1,2-*O*-isopropylidene-α-D-*xylo*-pentodialdo-1,4-furanose and K^{13}CN as described by King-Morris et al.[15] L-(6-^{13}C)Gulose was obtained from L-(6-^{13}C)idose by C2-epimerization with sodium molybdate.[16]

D-(6-^{13}C)Allose and L-(6-^{13}C)talose were prepared as described by King-Morris et al.[15] for the preparation of D-(6-^{13}C)glucose by substituting 1,2-*O*-isopropylidene-α-D-*ribo*-pentodialdo-1,4-furanose for 1,2-*O*-isopropylidene-α-D-*xylo*-pentodialdo-1,4-furanose as the starting sugar in the cyanohydrin reduction reaction. Epimerization of purified D-(6-^{13}C)allose and L-(6-^{13}C)talose with sodium molybdate[16] gave D-(6-^{13}C)-altrose and L-(6-^{13}C)galactose, respectively.

The labeled aldoses were identified by ^{13}C NMR spectroscopy using chemical shift data reported previously.[12]

Results and Discussion

A. Solution Properties of the Aldoses. Aqueous solutions of the C_4–C_6 aldoses contain several interconverting monomeric forms which include cyclic hemiacetals (pyranoses and/or furanoses) and acyclic *gem*-diol (hydrate) and aldehyde forms.[19,20] In general, acyclic forms are present in significantly lower abundance, and, when structurally allowed, pyranoses predominate over furanoses. The relative populations of these forms, and the kinetics of their interconversion, depend highly on aldose structure.[19-21] Thus, for example, aqueous solutions of D-glucose contain mainly pyranoses, whereas comparable amounts of furanose and pyranose forms are observed in aqueous solutions of D-talose[19,21b] and D-idose.[21c] In this study, we have restricted the examination of ^{13}C–^{13}C spin couplings to the more abundant cyclic forms.

In order to correlate ^{13}C–^{13}C spin couplings with molecular structure, it is essential to define the conformational behavior of each aldose. This behavior has been studied extensively for aldopyranoses,[5,22] which in general assume either $^4C_1$ or $^1C_4$ chair

(11) Barfield, M.; Walter, S. R. *J. Am. Chem. Soc.* **1983**, *105*, 4191.
(12) King-Morris, M. J.; Serianni, A. S. *J. Am. Chem. Soc.* **1987**, *109*, 3501.
(13) Serianni, A. S.; Barker, R. Synthetic Approaches to Carbohydrates Enriched with Stable Isotopes of Carbon, Hydrogen and Oxygen. In *Isotopes in the Physical and Biomedical Sciences*; Buncel, E., Jones, J. R., Eds.; Elsevier: New York, 1987; p 211.
(14) Serianni, A. S.; Vuorinen, T.; Bondo, P. B. *J. Carbohydr. Chem.* **1990**, *9*, 513.
(15) King-Morris, M. J.; Bondo, P. B.; Mrowca, R. A.; Serianni, A. S. *Carbohydr. Res.* **1988**, *175*, 49.
(16) Hayes, M. L.; Pennings, N. J.; Serianni, A. S.; Barker, R. *J. Am. Chem. Soc.* **1982**, *104*, 6764.
(17) Perlin, A. S. *Methods Carbohydr. Chem.* **1962**, *1*, 64.
(18) Serianni, A. S.; Nunez, H. A.; Barker, R. *Carbohydr. Res.* **1979**, *72*, 71.
(19) Angyal, S. J. *Angew. Chem., Int. Ed. Engl.* **1969**, *8*, 157.
(20) Angyal, S. J. *Adv. Carbohydr. Chem. Biochem.* **1984**, *42*, 15.
(21) (a) Serianni, A. S.; Pierce, J.; Huang, S.-G.; Barker, R. *J. Am. Chem. Soc.* **1982**, *104*, 4037. (b) Snyder, J. R.; Johnston, E. R.; Serianni, A. S. *J. Am. Chem. Soc.* **1989**, *111*, 2681. (c) Snyder, J. R.; Serianni, A. S. *J. Org. Chem.* **1986**, *51*, 2694.

Chart I

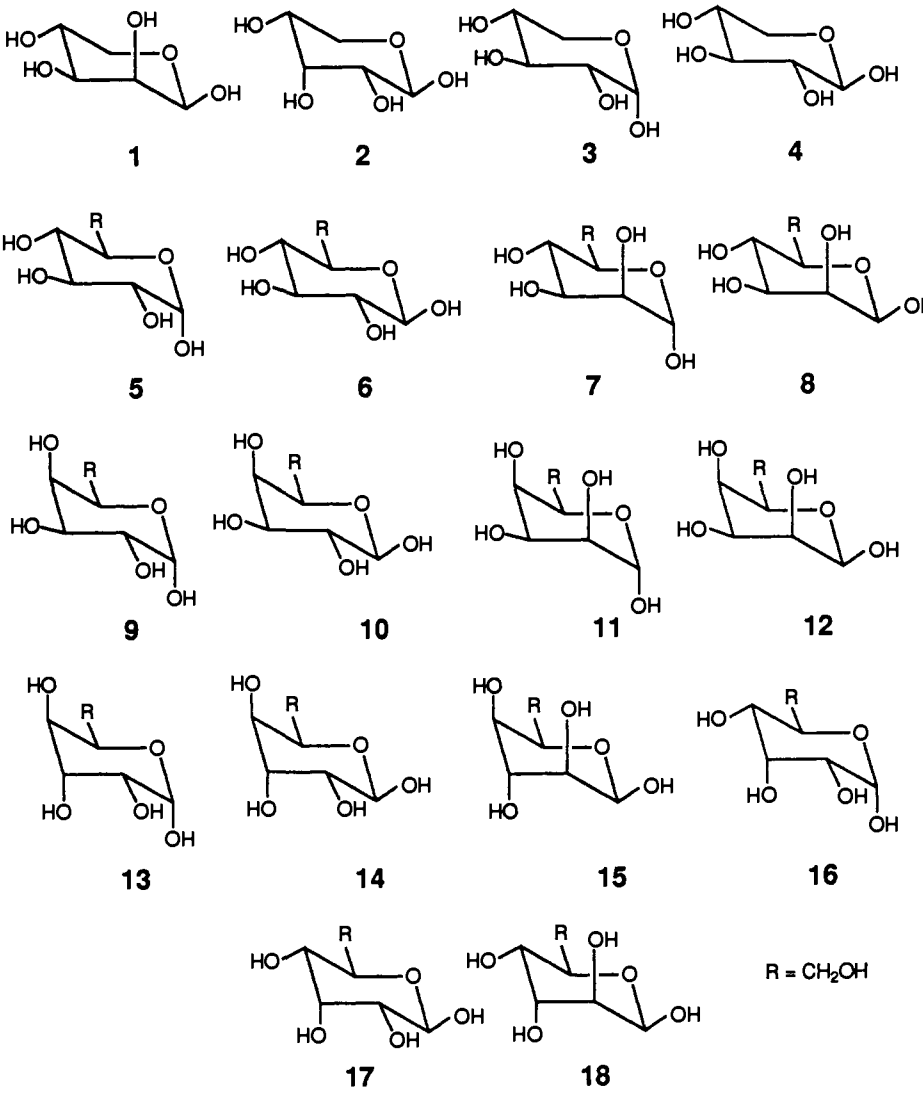

Chart II

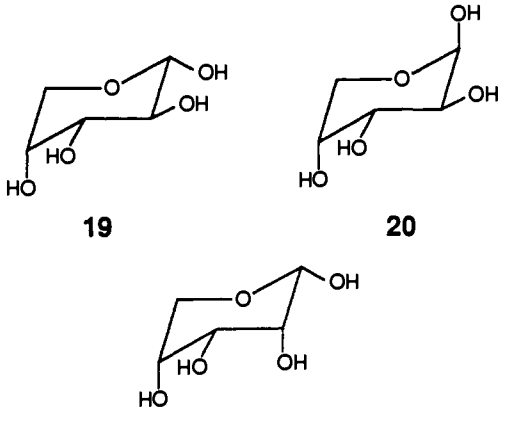

conformations. In the analysis below, the following aldopyranoses are considered to prefer the $^4C_1$ conformation (Chart I):[22b] β-D-lyxopyranose **1**, β-D-ribopyranose **2**, α-D-xylopyranose **3**, β-D-xylopyranose **4**, α-D-glucopyranose **5**, β-D-glucopyranose **6**, α-D-mannopyranose **7**, β-D-mannopyranose **8**, α-D-galactopyranose **9**, β-D-galactopyranose **10**, α-D-talopyranose **11**, β-D-talopyranose **12**, α-D-gulopyranose **13**, β-D-gulopyranose **14**, β-D-idopyranose **15**, α-D-allopyranose **16**, β-D-allopyranose **17**, and β-D-altropyranose **18**. Aldopyranoses preferring the $^1C_4$ conformation include α-D-arabinopyranose **19**, β-D-arabinopyranose **20**, and

Chart III

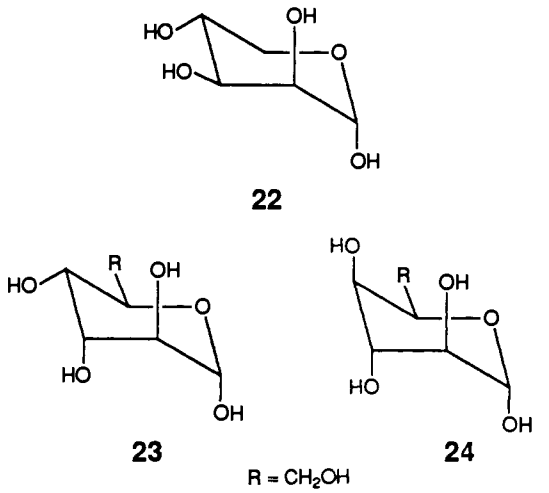

(22) (a) Eliel, E. L.; Allinger, N. L.; Angyal, S. J.; Morrison, G. A. *Conformational Analysis*; Interscience: New York, 1967; pp 351–432. (b) In Charts I–III and throughout this manuscript, all aldoses are represented in the D-configuration for consistency and to avoid confusion, despite the fact that in some cases ^{13}C–^{13}C couplings were measured in the mirror-image L-isomer (see Experimental Section). (c) Bock, K.; Pedersen, C. *Acta Chem. Scand. B* **1975**, *29*, 258.

Table I. $^{13}C-^{13}C$ Spin Couplings[a] in (6-^{13}C)Aldohexoses

compd	coupled nuclei C6,C5	C6,C4	C6,C3	C6,C1
	D-allose			
α-pyranose **16**	43.4	nc	2.8	3.2
β-pyranose **17**	43.1	nc	3.0	3.4
	D-altrose			
α-furanose	41.1	2.8	1.3	nc
β-furanose	41.2	2.3	2.0	nc
α-pyranose **23**	42.2	1.7	1.7	2.4
β-pyranose **18**	42.9	~0.6[b]	2.6	3.2
	D-galactose			
α-pyranose **9**	44.9	nc	3.7	3.6
β-pyranose **10**	44.6	nc	4.1	4.5
	D-glucose			
α-pyranose **5**	43.6	nc	3.9	3.3
β-pyranose **6**	43.0	nc	4.4	4.2
	D-gulose			
α-pyranose **13**	44.5	nc	1.8	3.4
β-pyranose **14**	44.5	nc	1.8	3.7
	D-idose			
α-furanose	40.8	3.5	~0.6[b]	nc
β-furanose	~41.5	2.8	1.4	nc
α-pyranose **24**	42.0	~0.7[b]	1.2	1.8
β-pyranose **15**	44.3	nc	2.1	3.0
	D-mannose			
α-pyranose **7**	43.3	nc	3.6	3.3
β-pyranose **8**	43.3	nc	4.2	3.9
	D-talose			
α-furanose	41.3	2.1	0.9	nc
β-furanose	41.8	1.3	2.3	nc
α-pyranose **11**	45.0	nc	3.4	3.4
β-pyranose **12**	45.0	nc	3.8	4.3

[a] In Hz. The entry "nc" denotes *no* coupling was observed ($J < \sim 0.8$ Hz). Coupling signs were not determined. For all entries, coupling between C2 and C6 was not observed. [b] Coupling observed in 1D INADEQUATE spectrum only.

Table II. $^{13}C-^{13}C$ Spin Couplings[a] in (5-^{13}C)Aldopentoses

compd	coupled nuclei C5,C4	C5,C3	C5,C2	C5,C1
	D-arabinose			
α-pyranose **19**	37.8	nc	nc	nc
β-pyranose **20**	37.5	nc	1.8	1.9
	D-lyxose			
α-pyranose **22**	38.9	nc	nc	1.5
β-pyranose **1**	39.6	1.7	nc	nc
	D-ribose			
α-furanose	42.4	1.3	1.1	1.9
β-furanose	42.0	1.8	1.8	nc
α-pyranose **21**	38.5	nc	br	0.8
β-pyranose **2**	39.7	nc	nc	0.9
	D-xylose			
α-pyranose **3**	39.1	0.9	nc	2.0
β-pyranose **4**	39.7	2.0	nc	nc

[a] In Hz. The entries "nc" and "br" denote *no* observed coupling ($J < \sim 0.8$ Hz) and *b*roadened signal, respectively. Coupling signs were not determined.

Table III. $^{13}C-^{13}C$ Spin Couplings[a] in (4-^{13}C)Aldotetroses

compd	coupled nuclei C4,C3	C4,C2	C4,C1
	D-erythrose		
α-furanose			nc
β-furanose		2.1	nc
hydrate			2.3
	D-threose		
α-furanose	37.2	1.6	nc
β-furanose	37.6	2.5	nc
hydrate			2.8

[a] In Hz. The entry "nc" denotes *no* observed coupling ($J < \sim 0.8$ Hz). No entry denotes couplings that were not measured. Coupling signs were not determined.

α-D-ribopyranose **21** (Chart II), while conformationally flexible aldoses (i.e., those whose $^4C_1$ and $^1C_4$ conformers have comparable stabilities or assume nonchair conformations) include α-D-lyxopyranose **22**, α-D-altropyranose **23**, and α-D-idopyranose **24** (Chart III).

The conformational preferences of the pentopyranoses (**1–4**, **19–22**) may be confirmed by examining the three-bond couplings between C5 and H1 ($^3J_{C5,H1}$) that are readily measured in the (5-^{13}C)derivatives. $^3J_{C5,H1}$ values obtained from high resolution 500 MHz ^1H NMR spectra of the (5-^{13}C)-enriched compounds are as follows: **1**, 1.7 Hz; **2**, 2.4 Hz; **3**, 6.5 Hz; **4**, 1.0 Hz; **19**, 0.9 Hz; **20**, 6.1 Hz; **21**, 2.5 Hz; **22**, 4.4 Hz. Standard $^3J_{C5,H1}$ values for dihedral angles of 60° and 180° are obtained from **4** (1.0 Hz) and **3** (6.5 Hz), respectively, since these structures are conformationally rigid ($^4C_1$ conformers).[19] A comparison of these standard values to $^3J_{C5,H1}$ observed in **19** and **20** indicates that pentopyranoses having the D-arabino configuration highly favor the $^1C_4$ conformation (Chart II). $^3J_{C5,H1}$ values for **1**, **2**, **21**, and **22** deviate from the standard values, indicating the presence of conformational heterogeneity (i.e., $^4C_1$ and $^1C_4$), although **1**, **2**, and **21** still favor one form, namely, $^4C_1$ for **1** (~87%) and **2** (~74%) (Chart I) and $^1C_4$ for **21** (~73%) (Chart II). The 4.4 Hz value of $^3J_{C5,H1}$ observed in **22** indicates that $^1C_4$ (~38%) and $^4C_1$ (~62%) conformers are present in comparable amounts in solution. These results are consistent with those obtained previously from an analysis of $^1J_{C1,H1}$ values.[22c]

$^{13}C-^{13}C$ spin coupling in aldofuranoses will also depend on ring conformation, but their interpretation is difficult since the conformational behavior of these rings is less well defined compared to that of pyranoses. However, as discussed below, the structure-coupling correlations derived from the examination of the more conformationally rigid pyranoses are valuable in interpreting related couplings in furanoses in terms of preferred ring and side-chain conformations.

B. Verification of ^{13}C Chemical Shifts in the Aldoses. Previous ^{13}C NMR studies of (1-^{13}C)-enriched aldoses at 75 MHz provided $^{13}C-^{13}C$ coupling data of importance in assessing the validity of reported ^{13}C signal assignments in these compounds.[12] The observation of one-bond $^{13}C-^{13}C$ couplings between C1 and C2 ($^1J_{C1,C2}$) provided an equivocal means to assign the C2 signals, and empirically derived structure-coupling correlations involving longer range couplings ($^2J_{C1,C}$ and $^3J_{C1,C}$) provided an auxiliary means to test many of the remaining assignments. The present study yielded new $^{13}C-^{13}C$ coupling information in these structures (Tables I–III), and a similar treatment of the data provided further confirmation of the reported assignments. These new data also resolved uncertainties in the assignments of the C3 and C4 signals of β-D-arabinopyranose **20**.[12] The observation of a large splitting of the signal at 70.2 ppm ($^1J_{C5,C4}$ = 37.5 Hz) and no splitting of the signal at 70.1 ppm allowed their firm assignment to C4 and C3, respectively.

In addition, the C5 signals of β-D-talofuranose and α-D-talopyranose were reported previously[21b] to be equivalent (72.6 ppm), but spectral data obtained on (6-^{13}C)talose show these signals resolved at 72.59 and 72.74 ppm, respectively. Chemical shift equivalence was also reported[12] for C4 of β-D-allopyranose and C5 of α-D-allopyranose (68.3 ppm), but the present data showed the latter signal to be 0.08 ppm downfield of the former. The C4 signals of the α- and β-D-gulopyranoses[12] were also resolved in spectra of the (6-^{13}C)-enriched sugar, occurring at 70.98 and 71.05 ppm, respectively. This improved resolution can be attributed to the enhanced signal dispersion at 125 MHz relative to that at 75 MHz.

C. $^{13}C-^{13}C$ Spin Coupling Constants. The measurement of $^{13}C-^{13}C$ spin coupling constants in (^{13}C)-enriched carbohydrates is sometimes complicated by the overlap of signals in crowded regions of the ^{13}C spectrum, especially for aldoses that exist in several interconverting forms in solution (e.g., ribose, altrose, idose, talose) and in complex structures such as oligosaccharides. This problem can sometimes be eliminated in INADEQUATE ^{13}C spectra of (^{13}C)-enriched compounds[12] either by selectively observing those carbons directly bonded to the enriched carbon or those further removed but still scalar coupled to the enriched site. This approach

Chart IV

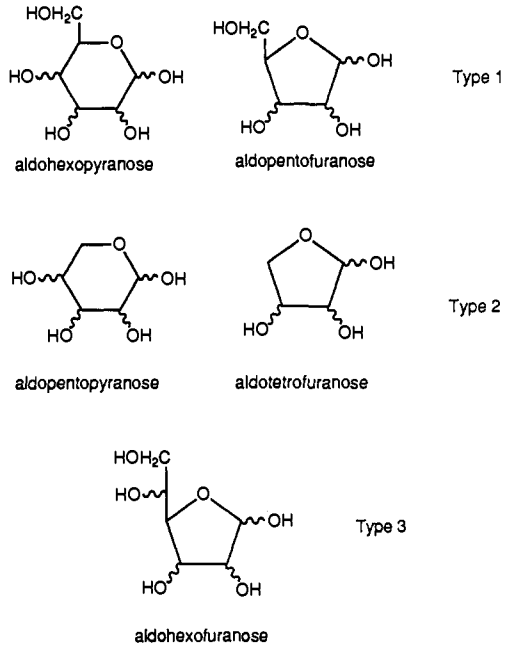

was used to assist spectral interpretation of several (6-^{13}C)aldoses and is illustrated for L-(6-^{13}C)idose in Figure 1. The detection of small ^{13}C–^{13}C couplings also appears to be enhanced in INADEQUATE spectra relative to conventional 1D spectra. The smallest detectable ^{13}C–^{13}C coupling observed in this study was 0.8 Hz, and thus the absence of an observed coupling ("nc" entries in Tables I–III) does not imply that $J = 0$ Hz but rather that $J < \sim 0.8$ Hz.

In this study, the signs of the observed couplings were not determined, although experimental methods to measure them have been reported.[8,23] and it is unlikely that all of the measured couplings have the same sign. The structure-coupling correlations developed below for $^1J_{CC}$ and $^3J_{CC}$ should be independent of coupling sign, however, since the signs of these couplings should remain constant. Some complications are encountered when interpreting $^2J_{CC}$ in the absence of sign information, as discussed in more detail below. In addition, while both through-bond and through-space mechanisms are believed to contribute to J_{CC},[8] no attempt has been made to evaluate their relative contributions to the observed couplings.

One-Bond J_{CC}. $^1J_{CC}$ involving the terminal (hydroxymethyl) carbon of the cyclic forms of the aldoses may be grouped into three types (Chart IV). The first (exo–endo) involves coupling between an exocyclic and an adjacent endocyclic carbon (e.g., C5 and C6 in aldohexopyranoses, C4 and C5 in aldopentofuranoses), the second (endo–endo) involves coupling between two endocyclic carbons (e.g., C5 and C4 in aldopentopyranoses, C4 and C3 in aldotetrofuranoses), and the third involves coupling between two exocyclic carbons (exo–exo) (e.g., C6 and C5 in aldohexofuranoses) (Chart IV). An examination of the data in Tables I–III reveals small differences in $^1J_{CC}$ for each type. $^1J_{C6,C5}$ (43.7 ± 1.0 Hz) and $^1J_{C5,C4}$ (42.2 ± 0.3 Hz) in aldohexopyranoses and aldopentofuranoses, respectively, are comparable in magnitude. In contrast, endo–endo $^1J_{C5,C4}$ (38.9 ± 0.9 Hz) and $^1J_{C4,C3}$ (37.4 ± 0.3 Hz) in aldopentopyranoses and aldotetrofuranoses, respectively, are similar in magnitude and 4–5 Hz smaller than exo–endo couplings. Exo–exo $^1J_{C6,C5}$ in aldohexofuranoses (41.3 ± 0.3 Hz) appear to be intermediate in magnitude. Thus, $^1J_{CC}$ may be a potential probe to distinguish between pyranose and furanose forms of an aldopentose but not of an aldohexose.

Two-Bond J_{CCC}. In aldohexopyranoses, no coupling is observed between C6 and C4 in all compounds except α-D-altropyranose **23** and α-D-idopyranose **24** (Table I). As a starting point in the structural interpretation of this result, we note that $^2J_{C1,C3}$ in aldopyranoses appears to depend in part on the relative orientation of the terminal hydroxyl oxygens, with maximum coupling (3.9–4.6 Hz) observed when O1 and O3 lie in the plane defined by C1, C2 and C3[12] (for example, in β-D-xylopyranose **4**). When one of these oxygens is displaced from this plane, $^2J_{C1,C3}$ is reduced to a very small or zero value.[24] When both oxygens are displaced from the plane, coupling is observed but is small (1–2 Hz) in magnitude.[12,25a] Previous studies of analogous two-bond ^{13}C–^1H couplings ($^2J_{CH}$) have indicated that oxygen substituents anti to the coupled proton make a positive contribution to the observed coupling, while oxygen substituents syn to the coupled proton make a negative contribution.[8] Thus, by analogy to these results, it is likely that $^2J_{C1,C3}$ has a positive sign when both O1 and O3 lie in the coupling plane and that displacing these oxygens out of this plane makes a negative contribution to the coupling and thus reduces its magnitude, as proposed by Marshall.[8] Thus, while the behavior of $^2J_{C1,C3}$ and $^2J_{C6,C4}$ in aldohexopyranoses may not be strictly analogous (i.e., in the former, two oxygens (O1 and O5) are appended to one of the coupled carbons (C1)), it may be postulated that the lack of an observed coupling between C6 and C4 in aldohexopyranoses is due to the fact that O4 is structurally forbidden to lie in the C6–C5–C4 plane in either $^4C_1$ or $^1C_4$ ring conformations. Under this structural constraint, and by analogy to the behavior of $^2J_{C1,C3}$,[12] coupling between C6 and C4 can only occur ($^4C_1$ conformers of D-isomers) when O6 is anti to O5 (if O4 is equatorial) or when O6 is anti to H5 (if O4 is axial). These hydroxymethyl conformations are destabilized by 1,3-interactions and are expected to be present in low abundance in solution. The presence of coupling between C4 and C6 in α-D-altropyranose **23** (1.7 Hz) is probably due to conformational heterogeneity; in the $^1C_4$ conformation, O4 lies in the C4–C5–C6 plane and coupling is expected. The presence of a small $^2J_{C6,C4}$ in **24** may also be due to the unusual conformational behavior of this hexose.[21c]

$^2J_{C5,C3}$ in aldopentopyranoses ranges in value from 0–2.0 Hz (Table II). Since the oxygen atom bonded to C5 is no longer a terminal substituent, the correlations observed for $^2J_{CC}$ above may not be valid for this coupling pathway. Indeed, if only the orientation of O3 is considered, no structure-coupling correlations are apparent. For example, O3 is equatorial (and thus in the C5–C4–C3 plane) in α- (**3**) and β- (**4**) D-xylopyranoses ($^4C_1$ conformers) and α- (**19**) and β- (**20**) D-arabinopyranoses ($^1C_4$ conformers), but coupling is observed only in the former. This observation suggests that the orientation of O4 relative to the ring oxygen may play a role in affecting $^2J_{C5,C3}$. This conclusion is supported by the observed values[25b] of $^2J_{C3,C5}$ in methyl β-D-glucopyranoside (2.5 Hz) and methyl β-D-galactopyranoside (1.4 Hz), where conversion of the intervening C4 hydroxyl group from an equatorial (anti to O5) to an axial (gauche to O5) position

(23) (a) Hansen, P. E.; Poulsen, O. K.; Berg, A. *Org. Magn. Reson.* **1975**, *7*, 405. (b) Linde, S. A.; Jakobsen, H. J. *J. Am. Chem. Soc.* **1976**, *98*, 1041. (c) Hansen, P. E.; Poulsen, O. K.; Berg, A. *Org. Magn. Reson.* **1976**, *8*, 632.

(24) An account should also be taken of the ring oxygen appended to C1 when interpreting $^2J_{C1,C3}$. Both oxygen substituents may be considered by inspecting the net dipole vector that bisects the O5–C1–O1 bond angle and lies in the O5–C1–O1 plane. This vector will be more closely aligned with the C1–C2–C3 plane in β-D-pyranoses than in α-D-pyranoses in the $^4C_1$ conformation. Therefore, an analysis of $^2J_{C1,C3}$ based on consideration of the relative orientations of only O1 and O3 along the coupling pathway, while not strictly correct, yields the same result.

(25) (a) The observed $^2J_{C1,C3}$ values in α-D-gulopyranose (2.0 Hz) and α-D-allopyranose (2.4 Hz) were attributed previously[12] to the presence of conformational averaging (i.e., $^4C_1$ and $^1C_4$). While averaging may be a factor, we now believe that a C1–C2–C3 coupling pathway having O1 and O3 in axial orientations may give rise to an observed $^2J_{C1,C3}$ that is smaller in magnitude (and perhaps different in sign) than $^2J_{C1,C3}$ for the same pathway in which O1 and O3 are equatorial. This contention is supported by the observation[28] that $^2J_{C2,C4} = 2.0$ Hz in α-D-talopyranose in which O2 and O4 lie in axial orientations. (b) Hayes, M. L.; Serianni, A. S.; Barker, R. *Carbohydr. Res.* **1982**, *100*, 87. (c) This effect is also observed for the C1–C2–C3 coupling pathway in aldohexopyranoses.[12] $^2J_{C1,C3} = 4.5$ Hz for β-D-glucopyranose (O2 equatorial), while $^2J_{C1,C3} \approx 4.0$ Hz for β-D-mannopyranose and β-D-talopyranose (O2 axial), indicating that hydroxyl orientation at the central C2 carbon influences the magnitude of this coupling. (d) Lemieux, R. U. *Molecular Rearrangements*; de Mayo, P., Ed.; Wiley-Interscience: New York, 1963; p 713.

reduces the value of this coupling constant. Thus, for $^2J_{CCC}$ the orientation of hydroxyl substituents on the central carbon relative to the terminal oxygens may influence the coupling magnitude.[25c] Furthermore, a significant difference in $^2J_{C5,C3}$ is observed between anomers of the conformationally rigid xylopyranoses (1.1 Hz; Table II), indicating that the electronic properties of the ring oxygen (which will be affected by O1 orientation due to the "anomeric effect"[25d]) may also influence this coupling in the aldopentopyranoses.

In aldohexofuranoses, $^2J_{C6,C4}$ ranges in value from 1.3 Hz (β-talofuranose) to 3.5 Hz (α-idofuranose) (Table I). In these structures, a zigzag extended coplanar O6–C6–C5–C4–O4 arrangement is structurally permitted and thus may partly explain the different behavior of $^2J_{C6,C4}$ in aldohexopyranoses and aldohexofuranoses. The relatively wide range of $^2J_{C6,C4}$ values in aldohexofuranoses probably reflects in part the different rotamer distributions for the two-carbon exocyclic fragment in these compounds, with larger values indicating a greater population of the rotamer having the above-noted coplanar arrangement (see discussion of $^3J_{C6,C3}$ below). It may be argued that the interpretation of $^2J_{C6,C4}$ in aldohexofuranoses suffers from the same problem encountered above for $^2J_{C5,C3}$ in aldopentopyranoses in that one of the oxygens along the coupling pathway is not a terminal substituent. We argue that this problem is not as critical for the former coupling. The effect of anomeric configuration on $^2J_{C6,C4}$ in aldohexofuranoses is likely to be much smaller since, on average, the C1–O1 bond prefers a quasiaxial orientation in aldofuranoses regardless of anomeric configuration. Furthermore, only one of the coupled carbons (C4) is near the anomeric center and thus under its influence, whereas for $^2J_{C5,C3}$ in aldopentopyranoses both C3 and C5, being ring carbons, are likely to be affected by structure at C1.

In contrast to $^2J_{C5,C3}$ in the aldopentopyranoses, $^2J_{C5,C3}$ in the aldopentofuranoses (Table II) is likely to be influenced by the same factors that affect this coupling in the aldohexopyranoses, since terminal oxygens are present in both cases. Thus, in the one case examined (ribofuranoses), coupling between C5 and C3 is observed (α, 1.3 Hz; β, 1.8 Hz). The conformations of the furanose ring and exocyclic hydroxymethyl fragment are expected to play an important role in determining $^2J_{C5,C3}$ in the aldopentofuranoses. For example, coupling might be expected in the ^{4}E conformers of D-ribopentofuranoses (and D-arabinopentofuranoses) in which both O3 and O5 (*gt* hydroxymethyl conformation) may lie in the C5–C4–C3 plane. Thus, the magnitude of $^2J_{C5,C3}$ may have potential applications in the conformational analysis of pentofuranoses. This reasoning allows for the prediction that $^2J_{C5,C3}$ in aldopentofuranoses having the lyxo and xylo configurations should be small or zero, since structural constraints prevent O3 from lying in the zigzag extended O5–C5–C4–C3 plane in all furanose conformers having these ring configurations. This prediction remains to be tested experimentally.

Coupling between C4 and C2 of aldotetrofuranoses (Table III) cannot be easily interpreted, as this coupling ($^{2+3}J_{C4,C2}$) will be determined by two pathways, namely, C4–O4–C1–C2 and C4–C3–C2. In the structures studied, this coupling ranges in magnitude from 1.6 to 2.5 Hz. $^{2+3}J_{C4,C1}$ in aldotetrofuranoses is also determined by two pathways (C4–O4–C1 and C4–C3–C2–C1) as discussed previously in a study of (1-^{13}C)tetrofuranoses.[26] In the cases studied to date, $^{2+3}J_{C4,C1}$ is usually small or zero in furanose rings, in contrast to $^{2+3}J_{C4,C2}$.

Three-Bond J_{CCCC}. Coupling between C6 and C3 in the aldohexopyranoses will depend in part on the dihedral angle, θ, between these sites, that is, on the C5–C4 torsion angle. However, other factors such as the nature and geometry of substituents along the coupling pathway can have a notable effect on vicinal ^{13}C–^{13}C couplings. The latter effect was probed systematically by comparing $^3J_{C6,C3}$ in the aldohexopyranoses having defined ring conformations.

Four structural motifs for the C6–C5–C4–C3 coupling pathway are available in the conformationally rigid (^{4}C$_1$) D-aldohexopyranoses in which C6 and C3 are fixed in an antiperiplanar geometry ($\theta \approx 180°$) (Chart V). These motifs are distinguished by the relative orientation of O3 and O4 (O5 is present in a fixed geometry in all compounds). An examination of the data in Table I shows that coupling between C6 and C3 in aldohexopyranoses having these atoms oriented antiperiplanar is notably affected by the relative geometry of the hydroxyl substituents along the coupling pathway. Coupling is maximal when O3 and O4 are equatorial (3.6–4.4 Hz in glucopyranoses **5** and **6** and mannopyranoses **7** and **8**) or when O3 is equatorial and O4 is axial (3.4–4.1 Hz in galactopyranoses **9** and **10** and talopyranoses **11** and **12**) and minimal when these substituents are axial (1.8 Hz in gulopyranoses **13** and **14**) (Chart V). Intermediate values are observed when O3 is axial and O4 is equatorial (2.6–3.0 Hz in allopyranoses **16** and **17** and β-altropyranose **18**) (Chart V). Thus, while the dihedral angle between C6 and C3 is constant or nearly so ($\sim$180°), the observed coupling ranges in magnitude from 1.8–4.4 Hz depending on pathway structure. Failure to appreciate this effect could lead to erroneous interpretations of $^3J_{C6,C3}$ in carbohydrates, as in the absence of this knowledge a 1.8 Hz coupling might be interpreted as originating from carbons oriented gauche or near gauche ($\theta \approx 60°$). It should also be noted that the orientation of O6 with respect to the coupling pathway may effect $^3J_{C6,C3}$, with an in-plane position (*gt* conformer) enhancing coupling, but this effect could not specifically be evaluated due to the rotational properties of the C5–C6 bond. This factor, however, may account for the observed difference in $^3J_{C6,C3}$ between pyranose anomers (e.g., 3.9 Hz in α-D-glucopyranose **5**, 4.4 Hz in β-D-glucopyranose **6**). Thus, the different magnitudes of $^3J_{C6,C3}$ between aldohexopyranose anomers having similar ring conformations may reflect differences in the distribution of C5–C6 rotamers.

Chart V

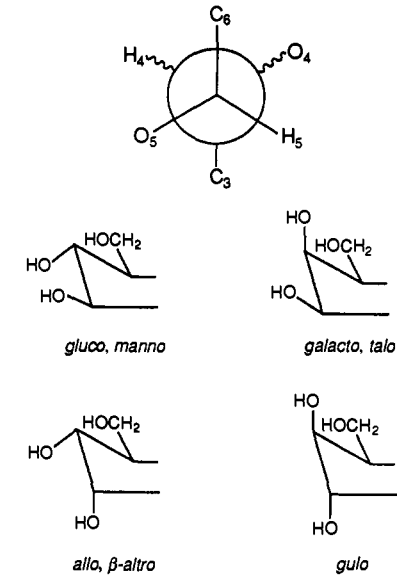

In addition to the above-noted effect of hydroxyl substituents along a vicinal ^{13}C–C–C–^{13}C coupling pathway, dihedral angle also affects $^3J_{C6,C3}$ as expected. This effect is illustrated by the 1.2 Hz coupling observed in α-D-idopyranose **24**, which prefers a ^{1}C$_4$ or related skew conformation[21c] in which C6 and C3 are oriented gauche or near gauche. The corresponding dihedral angle ($\theta \approx 60°$) should yield a smaller coupling than is observed when $\theta \approx 180°$. The presence of conformational heterogeneity is also likely to be responsible for the small $^3J_{C6,C3}$ in α-D-altropyranose (1.7 Hz).

$^3J_{C6,C3}$ in the aldohexofuranoses (Table I) is expected to show a structural dependency similar to that for $^3J_{C6,C3}$ in the aldohexopyranoses, although this dependency is difficult to assess due to the rotational properties of the exocyclic two-carbon fragment and the conformational mobility of the furanose ring. However, it is interesting to compare the *relative magnitudes* of $^2J_{C6,C4}$ and

(26) Serianni, A. S.; Barker, R. *J. Org. Chem.* **1984**, *49*, 3292.

Chart VI

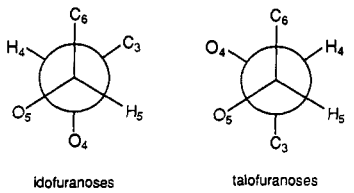

$^3J_{C6,C3}$, as both parameters will be affected differently, and in a complementary fashion, by the C4–C5 torsion angle. If we assume that hydroxyl orientational effects along the coupling pathway are small or cancel in this comparison, then $^3J_{C6,C3}$ should be large and $^2J_{C6,C4}$ should be small when C6 and C3 are antiperiplanar, as the former coupling is enhanced when C6 and C3 are antiperiplanar while the latter is enhanced when C6 and C3 are gauche (i.e., C6 and O4 are antiperiplanar) (see discussion of $^2J_{CC}$ above). This inverse relationship in the magnitudes of $^2J_{C6,C4}$ and $^3J_{C6,C3}$ in the aldohexofuranoses appears to be observed in the compounds studied (Table I). Data in Table I indicate that $^2J_{C6,C4} > {}^3J_{C6,C3}$ in the idofuranoses while $^2J_{C6,C4} < {}^3J_{C6,C3}$ in β-D-talofuranose, suggesting that the distribution of rotamers about the C4–C5 bond in these structures differs significantly. $^3J_{H4,H5}$ values should reflect this difference and have been reported to be larger in idofuranoses (~7.5 Hz)[27] than in β-D-talofuranose (3.2 Hz).[21b] The large value of $^3J_{H4,H5}$ in the former indicates a greater preference for the C4–C5 rotamer having these atoms antiperiplanar (Chart VI), and this conformation is consistent with the observed *relative* magnitudes of $^2J_{C6,C4}$ and $^3J_{C6,C3}$ in these structures. The smaller $^3J_{H4,H5}$ in β-D-talofuranose suggests that H4 and H5 prefer to be oriented gauche in these structures, and, of the two gauche conformers available, that having C6 and C3 antiperiplanar appears to be preferred (Chart VI) based on the large magnitude of $^3J_{C6,C3}$ relative to $^2J_{C6,C4}$. Thus, internal consistency in the conformational interpretation of ^1H–^1H and ^{13}C–^{13}C couplings in the exocyclic two-carbon fragment of these aldohexofuranoses is obtained, but additional studies will be needed to further validate these observations.

In the pentopyranoses, coupling between C5 and C2 ($^{3+3}J_{C5,C2}$) will be determined by two three-bond coupling pathways (C5–C4–C3–C2 and C5–O5–C1–C2), and coupling is observed in only one case (1.8 Hz in **20**, Table II). Similar behavior was observed previously[12] for the related $^{3+3}J_{C1,C4}$ in the aldohexopyranoses.

Couplings between Terminal Hydroxymethyl Carbons and C1 in Aldopentoses and Aldohexoses. These couplings have been studied previously using (1-^{13}C)-enriched aldoses[12] and thus are not discussed here. In two cases (D-ribopyranoses and D-mannopyranoses), however, coupling to the terminal carbons could not be determined with (1-^{13}C)-enriched compounds due to resonance overlap. This problem was resolved by observing the coupling in the reverse direction (Tables I and II), and the observed values are consistent with the structure-coupling correlations derived previously.[12]

Conclusions

Carbohydrates provide a convenient conformationally-defined and readily substituted carbon scaffolding to assess the effect of coupling pathway structure on the magnitudes of one-bond and longer range ^{13}C–^{13}C coupling constants. Of particular interest is not only the nature of the substituents along the coupling pathway (electronegative hydroxyl groups in the present study, although other substituents could be incorporated) but also their relative configuration. The aim of this investigation was to study the complete set of simple aldotetroses, aldopentoses and aldohexoses in order to obtain sufficient coupling data to derive empirical structure-coupling correlations. An understanding of these correlations will assist in the application of these couplings to carbohydrate structure and conformational analysis and will be valuable for future theoretical (i.e., calculational) studies of ^{13}C–^{13}C coupling in these molecules.

$^1J_{CC}$ involving the terminal hydroxymethyl aldose carbon is moderately sensitive to the nature of the coupled carbons, that is, whether one or both carbons is endocyclic or exocyclic. The observed effect may be mainly attributed to differences in the *s*-character of the carbon–carbon bond, the latter being affected by the substituents appended to the coupled carbons.

The longer range J_{CC}, however, are highly affected by coupling pathway geometry. For $^2J_{CCC}$ in which the coupled carbons are bonded to hydroxyl groups, we found that coupling is large for O–C–C–C–O fragments having a zigzag extended planar geometry. Thus, for β-D-pyranoses ($^4C_1$ conformers), $^3J_{C1,C3}$ is large while $^2J_{C1,C3}$ in α-D-pyranoses is small or zero.[12] On the basis of these previous observations, the small or zero value of $^2J_{C6,C4}$ in most aldohexopyranoses is not surprising, as the covalent structure of these rings prevents the O6–C6–C5–C4–O4 fragment from assuming the extended geometry required for coupling to occur. It is clear that the terminal oxygen substituents along the two-bond ^{13}C–C–^{13}C coupling pathway have a significant impact on the magnitude of the observed coupling. On the basis of the above observations, it may be predicted that $^2J_{C2,C4}$ in glucopyranoses should be much larger than $^2J_{C2,C4}$ in mannopyranoses and galactopyranoses. Indeed, recent studies of (2-^{13}C)aldohexoses[28] show that $^2J_{C2,C4}$ = 3.0 Hz for α-D-glucopyranose **5** and 2.8 Hz for β-D-glucopyranose **6**, whereas no coupling is observed between C2 and C4 in the α- and β-pyranoses having the D-manno and D-galacto configurations, in agreement with prediction. It should be appreciated, however, that the analysis of $^2J_{CC}$ presented in this paper is based on a relatively small data set and that further study involving the measurement of coupling signs is likely to result in further modification and refinement of rules correlating carbohydrate structure with the magnitudes of these couplings.

$^3J_{CCCC}$ is highly affected by dihedral angle and substituent geometry. A comparison of several conformationally-rigid aldohexopyranoses having C6 and C3 in an anti orientation has clearly shown that axial hydroxyl substituents truncate $^3J_{C6,C3}$ and that the effect is roughly additive. $^3J_{C6,C3}$ values may differ by a factor of 2 for coupled carbons related by the same 180° dihedral angle, depending on the relative configuration of the hydroxyl groups appended to the terminal *and* intervening carbons along the coupling pathway. This dependency serves to reemphasize the fact that care must be taken when interpreting $^3J_{CC}$ in terms of molecular conformation, especially when structure-coupling relationships pertinent to the specific coupling pathway in question are not fully appreciated.

This study has also suggested potential new applications of some ^{13}C–^{13}C couplings to problems in carbohydrate structure elucidation. For example, the complementarity in the magnitudes of $^2J_{C6,C4}$ and $^3J_{C6,C3}$ in aldohexofuranosyl rings may be useful in assessing exocyclic conformation in these compounds, but further study will be needed to confirm their utility in this regard.

Acknowledgment. This work was supported by the National Institutes of Health (GM 33791) and Omicron Biochemicals, Inc.

Registry No. D-**1**, 139657-44-6; D-**2**, 139657-45-7; D-**3**, 139657-46-8; D-4, 139703-78-9; D-**5**, 65718-33-4; D-**6**, 65718-34-5; D-**7**, 139756-87-9; D-**8**, 139756-88-0; L-**9**, 139756-89-1; L-**10**, 139756-90-4; L-**11**, 139756-91-5; L-**12**, 139756-92-6; L-**13**, 139756-93-7; L-**14**, 139756-94-8; L-**15**, 139756-95-9; D-**16**, 139756-96-0; D-**17**, 139756-97-1; D-**18**, 139756-98-2; D-**19**, 139657-47-9; D-**20**, 139657-48-0; D-**21**, 139657-49-1; D-**22**, 139657-50-4; D-**23**, 139756-99-3; L-**24**, 139757-00-9; β-D-(4-^{13}C)-erythrofuranose, 139657-51-5; D-(4-^{13}C)erythrose hydrate, 139657-52-6; D-(4-^{13}C)erythrose, 90913-08-9; α-D-(4-^{13}C)threofuranose, 139657-53-7; β-D-(4-^{13}C)threofuranose, 139657-54-8; D-(4-^{13}C)threose hydrate, 139657-55-9; D-(4-^{13}C)threose, 139657-64-0; D-(6-^{13}C)allose, 139657-56-0; D-(6-^{13}C)altrose, 139657-57-1; L-(6-^{13}C)galactose, 139657-58-2; D-(6-^{13}C)glucose, 70491-70-2; L-(6-^{13}C)gulose, 115973-82-5; L-(6-^{13}C)-idose, 115973-80-3; D-(6-^{13}C)mannose, 115973-81-4; L-(6-^{13}C)talose, 139657-59-3; D-(5-^{13}C)arabinose, 139657-60-6; D-(5-^{13}C)lyxose, 139657-61-7; D-(5-^{13}C)ribose, 139657-62-8; D-(5-^{13}C)xylose, 139657-63-9; 1,2-*O*-isopropylidene-α-D-*xylo*-pentodialdo-1,4-furanose, 53167-11-6; 1,2-*O*-isopropylidene-α-D-*ribo*-pentodialdo-1,4-furanose, 63846-98-0.

(27) Schwarcz, J. A.; Perlin, A. S. *Can. J. Chem.* **1972**, *50*, 3667.

(28) Wu, J.; Serianni, A. S., unpublished results.